Current density in a long solitary tubular conductor

2008 J. Phys. A: Math. Theor. 41 145401

(http://iopscience.iop.org/1751-8121/41/14/145401)

J. Phys. A: Math. Theor. **41** (2008) 145401 (14pp) doi:10.1088/1751-8113/41/14/145401

Current density in a long solitary tubular conductor

O Coufal

Faculty of Electrical Engineering and Communication, Brno University of Technology, Technická 8, 616 00 Brno, Czech Republic

E-mail: coufal@feec.vutbr.cz

Received 4 January 2008, in final form 12 February 2008
Published 26 March 2008
Online at stacks.iop.org/JPhysA/41/145401

Abstract

Two models are described whose solution is the current density in a tubular conductor that is given by the radii $r_i < r_o$ and supplied from an ideal current source of a frequency that does not exceed 1 GHz. It has been proven that the two models are equivalent, but model 1 can practically be used only to calculate current density in a cylindrical conductor ($r_i = 0$). The general methods proposed are applied to several concrete examples of tubular and cylindrical conductors. The solution of examples is given in the figures. In the solution of examples, attention is devoted to problems that are connected with the realization of numerical calculation on a computer.

PACS numbers: 41.20.−q, 02.60.−x, 84.32.Ff

1. Introduction

Consider a solitary massive conductor of infinite length whose cross-section is in the shape of annular area. The longitudinal axis of the conductor is axis z of the system of Cartesian coordinates xyz. In addition to the xyz coordinates, the system cylindrical coordinates $r\phi z$ is also considered. Because of the symmetry with respect to axis z, the ϕ coordinate will not be used in the following. The conductor cross-section in the xy plane is determined by the inequalities $r_i \leqslant r \leqslant r_o, r_i \geqslant 0$. The conductor is connected to an ideal current source [1] whose current only depends on time $t \in [0, \infty)$. The ideal current source supplies current, but the current does not flow through the source so that no back conductor to the tube under examination needs to be considered [2]. This case differs substantially from the case solved in [3, 4], where the existence of a back conductor is assumed. The current density vector $\boldsymbol{J}$ is in the direction of axis z and only depends on r and t. $\boldsymbol{J} = (0, 0, J)$, with $J = J(r, t)$ having a non-zero value only on the interval $[r_i, r_o]$. The current flowing through the conductor excites a magnetic field that is determined by the vector $\boldsymbol{B}$ or $\boldsymbol{H}$, whose magnitude B or H also depends on only r and t. The fact that $\boldsymbol{J}$, $\boldsymbol{B}$ and $\boldsymbol{H}$ do not depend on z actually means that an infinitely high propagation velocity of an electromagnetic field is assumed. In such a

case, the current is considered to be slowly varying [5]. We assume that the permeability of the conductor and its environs is μ_0. The conductor resistivity ϱ is so low that displacement current $\partial \boldsymbol{D}/\partial t$ can be neglected. In the whole of this paper the part of the conductor between the planes $z = z_1$ and $z = z_2$, where $z_1 < z_2$, $z_2 - z_1 = z_{21}$, will be considered.

The magnetic field of a current flowing through a tubular conductor is easy to determine using Ampere's circuital law [5, 6]:

$$\oint_C \boldsymbol{H} \cdot \mathrm{d}\boldsymbol{C} = \int_{A_C} \boldsymbol{J} \cdot \mathrm{d}\boldsymbol{A}_C, \tag{1}$$

where C is a simple finite closed curve that is smooth by parts [7], the only curve in the following, and A_C is a simple finite surface that is smooth by parts [7], the only surface in the following, bounded by the curve C. Current from the current source is affected in the conductor by currents that are induced in the conductor according to Faraday's law of electromagnetic induction. According to this law, in every closed curve C whose position and shape do not depend on t electromotive force is induced:

$$\mathrm{emf}_C = \oint_C \boldsymbol{E} \cdot \mathrm{d}\boldsymbol{C} = -\frac{\partial \Phi}{\partial t}, \tag{2}$$

where $\boldsymbol{E}$ is the vector of the electric field, and

$$\Phi = \int_{A_C} \boldsymbol{B} \cdot \mathrm{d}\boldsymbol{A}_C$$

is a magnetic flux linking the curve C, which does not depend on the shape of surface A_C [5]. In addition to the validity of relations (1) and (2), we will further assume that it holds

$$\boldsymbol{J} = \gamma \boldsymbol{E}, \qquad \text{where} \quad \gamma = \frac{1}{\varrho}, \tag{3}$$

$$\nabla \cdot \boldsymbol{J} = 0, \tag{4}$$

$$\boldsymbol{B} = \mu_0 \boldsymbol{H}, \tag{5}$$

$$\nabla \cdot \boldsymbol{B} = 0.$$

2. Current density in a tubular conductor

The cylindrical conductor is a special case of the conductor under consideration for $r_\mathrm{i} = 0$. The method for calculating the current density in a cylindrical conductor was first proposed by Maxwell; it is given, for example, in [8]. Two models will be described below, whose solution is the current density in a tubular conductor supplied by an ideal current source.

2.1. Model 1

To derive model 1 we will, in principle, use the procedure proposed in [8]. The starting point is relation (1) and relation (2) in the differential form

$$\nabla \times \boldsymbol{H} = \boldsymbol{J}, \tag{6}$$

$$\nabla \times \boldsymbol{E} = -\frac{\partial \boldsymbol{B}}{\partial t}. \tag{7}$$

Using (6), equation (5) can be arranged to the form

$$\nabla \times \boldsymbol{B} = \mu_0 \boldsymbol{J}. \tag{8}$$

With the aid of (3), we will substitute for $\boldsymbol{E}$ in (7). After applying the rotation operation to (7) we will, with the help of (8), obtain

$$\nabla \times \nabla \times \boldsymbol{J} = -\gamma \frac{\partial}{\partial t} \nabla \times \boldsymbol{B}.$$

In re-writing this equation, we take into consideration (4) and (8) and obtain

$$\nabla^2 \boldsymbol{J} - \mu_0 \gamma \frac{\partial \boldsymbol{J}}{\partial t} = 0. \tag{9}$$

The conductor is symmetrical with respect to axis z, and so $\boldsymbol{J}$ only depends on r and t, and its only non-zero component is J_z. Model 1 is equation (9) written for the component J_z alone.

For a conductor supplied by sinusoidal current

$$J_z = \hat{J}(r) \sin\left[\omega t + \alpha(r)\right],$$

equation (9) can be solved for complex current density

$$\underline{J} \exp(\mathrm{j}\omega t), \quad \text{where } \underline{J} = \hat{J}(r) \exp(\mathrm{j}\alpha(r)).$$

Substituting complex current density for $\boldsymbol{J}$ in (9) will, after minor re-writing, yield the equation

$$\frac{\mathrm{d}^2 \underline{J}}{\mathrm{d}r^2} + \frac{1}{r} \frac{\mathrm{d}\underline{J}}{\mathrm{d}r} - \mathrm{j}\kappa^2 \underline{J} = 0, \qquad \kappa^2 = \omega \mu_0 \gamma, \tag{10}$$

which phasor $\underline{J}$ must satisfy. In addition to r, consider also the independent variable

$$x = \kappa r, \qquad x \in [\kappa r_\mathrm{i}, \kappa r_\mathrm{o}]. \tag{11}$$

It holds

$$\frac{\mathrm{d}\underline{J}}{\mathrm{d}r} = \kappa \frac{\mathrm{d}\underline{J}}{\mathrm{d}x}, \qquad \frac{\mathrm{d}^2 \underline{J}}{\mathrm{d}r^2} = \kappa^2 \frac{\mathrm{d}^2 \underline{J}}{\mathrm{d}x^2}.$$

We will restrict ourselves to $r > 0$, i.e. $r_\mathrm{i} > 0$. On this assumption, we can multiply equation (10) by r^2. Using (11) we express r and obtain the Kelvin differential equation [9]

$$x^2 \frac{\mathrm{d}^2 \underline{J^x}}{\mathrm{d}x^2} + x \frac{\mathrm{d}\underline{J^x}}{\mathrm{d}x} - \mathrm{j}x^2 \underline{J^x} = 0, \tag{12}$$

where

$$\underline{J^x} = \underline{J^x}(x) = \underline{J}\left(\frac{x}{\kappa}\right).$$

By [7], the general solution of equation (12) is

$$\underline{J^x}(x) = c_B[\mathrm{ber}(x) + \mathrm{j}\,\mathrm{bei}(x)] + c_K[\mathrm{ker}(x) + \mathrm{j}\,\mathrm{kei}(x)], \tag{13}$$

with Kelvin functions $\mathrm{ber}(x)$, $\mathrm{bei}(x)$, $\mathrm{ker}(x)$ and $\mathrm{kei}(x)$ defined, for example, in [7], and the constants c_B and c_K determined by initial conditions.

2.2. Model 2

When formulating model 2, the starting point is relations (1), (2) and Kirchhoff's voltage law. Unlike in model 1, in model 2 it is not necessary to assume that $r_\mathrm{i} > 0$; there can also be $r_\mathrm{i} = 0$. We choose division D_n of the interval $[r_\mathrm{i}, r_\mathrm{o}]$ with the aid of points $r_0 < r_1 < r_2 < \cdots < r_n$, with $r_0 = r_\mathrm{i}$ and $r_n = r_\mathrm{o}$. We assume that for $k = 1, 2, \ldots, n$, D_n satisfies the condition

$$a = \pi\left(r_k^2 - r_{k-1}^2\right), \qquad \text{where} \quad a = \frac{\pi\left(r_\mathrm{o}^2 - r_\mathrm{i}^2\right)}{n}.$$

By means of the division D_n we can divide the conductor into n partial conductors, with the cross-section of the kth conductor being an annulus determined by the circles $r = r_{k-1}$ and

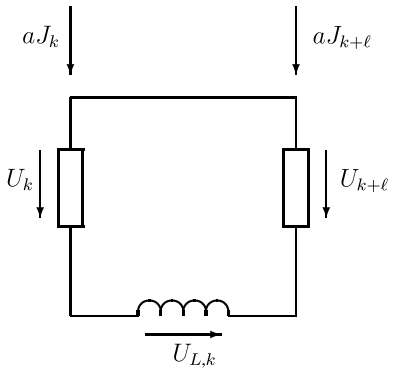

Figure 1. Substitute circuit of a loop formed by the kth and $(k+\ell)$th partial conductors between the planes $z = z_1$ and $z = z_2$.

$r = r_k$. The conductor resistivity is constant and therefore the current density in the conductor will be continuous with respect to r and thus it can at any instant of time be approximated with arbitrary precision by a function that is constant by parts such that in the kth partial conductor its magnitude is $J_k(t)$, independent of r. A current $aJ_k(t)$ flows through the kth partial conductor. The kth and $(k+\ell)$th partial conductors ($\ell > 0$) between the planes $z = z_1$ and $z = z_2$ can be replaced by a lumped-elements circuit; the schematic diagram of the circuit is given in figure 1. The number of such (mutually different) circuits is $n(n-1)/2$, but there are only $n-1$ independent circuits among them. Using the independent circuits, all potential circuits can be created. In the following, we will therefore consider only independent circuits for $\ell = 1$. For the kth independent circuit, it holds by Kirchhoff's law

$$U_{k+1}(t) - U_k(t) - U_{L,k}(t) = 0, \qquad k = 1, 2, \ldots, n-1, \tag{14}$$

where $U_{L,k}$ is the voltage induced in the kth circuit and U_k and U_{k+1} are voltages across the resistances that substitute the respective partial conductors. It holds

$$U_{k+1} - U_k = \varrho z_{21}(J_{k+1} - J_k). \tag{15}$$

Let us choose the points $c_1 < c_2 < \cdots < c_n$ such that $r_{k-1} \leqslant c_k \leqslant r_k$. Let us denote

$$\widetilde{U}_{L,k} = \frac{\partial \Phi}{\partial t}, \qquad \Phi = \int_{A_C} \boldsymbol{B} \cdot \mathrm{d}\boldsymbol{A}_C,$$

with A_C being a rectangle $S_k = [c_k, c_{k+1}] \times [z_1, z_2]$ in the plane $y = 0$ and the curve C the boundary of this rectangle. If we take into consideration the fact that the magnetic field $\boldsymbol{B}$ excited by the current in the conductor under consideration has on the circle $r = \text{const}$ the direction of the tangent to this circle, then it follows from the above that

$$\widetilde{U}_{L,k}(t) = z_{21} \frac{\partial}{\partial t} \left(\sum_{\ell=1}^{n} J_\ell(t) \int_{c_k}^{c_{k+1}} \mathscr{B}_\ell(r) \mathrm{d}r \right), \tag{16}$$

where $\mathscr{B}_\ell(r)$ is a magnetic field excited by the ℓth partial conductor per unit current density, i.e. $\mathscr{B}_\ell(r)$ is expressed in Wb A^{-1}. The quantity $\mathscr{B}_\ell(r)$ is easy to calculate using (1). For given $c_1, c_2, \ldots, c_n$, the magnetic fluxes considered depend on t alone. The function $J_\ell(t)$ on the right-hand side of relation (16) also depends on t alone, and therefore the derivative $\partial/\partial t$ can be replaced by the derivative $\mathrm{d}/\mathrm{d}t$.

For a sufficiently large n the electromotive force $\widetilde{U}_{L,k}$ induced around the boundary of the rectangle S_k differs little from the voltage $U_{L,k}$ induced in the kth circuit so that using (15), (16) and (3), equation (14) is in the form

$$J_{k+1}(t) - J_k(t) - \gamma \sum_{\ell=1}^{n} \Phi_{k\ell} \frac{\mathrm{d}}{\mathrm{d}t} J_\ell(t) = 0, \qquad k = 1, 2, \ldots, n-1, \tag{17}$$

where

$$\Phi_{k\ell} = \int_{c_k}^{c_{k+1}} \mathscr{B}_\ell(r)\, \mathrm{d}r.$$

Relation (17) is a system of $n-1$ ordinary differential equations for unknown functions $J_k(t), k = 1, 2, \ldots, n$. These functions cannot be determined by means of (17) because the number of unknowns is by one greater than the number of equations; in the following, we therefore distinguish between model 2I and model 2J.

In model 2I, we add to equation (17) the equation

$$a \sum_{\ell=1}^{n} J_\ell = I, \tag{18}$$

where I is the chosen current flowing through the conductor. Model 2I is a system of differential-algebraic equations [10] formed by a system of differential equations (17) extended by algebraic equation (18).

Model 2J will be obtained by choosing one of the current densities $J_k(t), k = 1, 2, \ldots, n$, such that it is non-zero, for example $J_s(t)$. After substituting the chosen current density into (17), this system will change to a system of $n-1$ non-homogeneous differential equations for unknown functions $J_1(t), J_2(t), \ldots, J_{s-1}(t), J_{s+1}(t) \ldots, J_n(t)$.

For a conductor supplied by sinusoidal current, the current density or the complex current density in the kth partial conductor will be

$$J_k(t) = \hat{J}_k \sin(\omega t + \alpha_k) \tag{19}$$

or

$$\underline{J_k} \exp(\mathrm{j}\,\omega t), \qquad \text{where} \quad \underline{J_k} = \hat{J}_k \exp(\mathrm{j}\,\alpha_k).$$

For the complex current density, (17) can be rewritten as a system of equations

$$\underline{J_{k+1}} - \underline{J_k} - \mathrm{j}\,\omega\gamma \sum_{\ell=1}^{n} \Phi_{k\ell} \underline{J_\ell} = 0, \qquad k = 1, 2, \ldots, n-1. \tag{20}$$

In model 2I (20) will be extended by equation (18) written for the respective phasors. This will yield a system of n linear non-homogeneous equations for phasors $\underline{J_1}, \underline{J_2}, \ldots, \underline{J_n}$. We obtain model 2J by choosing one of these phasors and substituting it in (20). A normalized model 2J is obtained by normalizing equations (20), i.e. dividing them by one of the phasors, e.g. $\underline{J_s}$. Normalized phasors

$$\underline{J_k}_{\mathrm{rel}} = \frac{\underline{J_k}}{\underline{J_s}}, \qquad k = 1, 2, \ldots, s-1, s+1, \ldots, n,$$

are the solution of normalized system (20), and $\underline{J_s}_{\mathrm{rel}} = 1$.

3. Comparison of the two models

Zero current density satisfies system (17) and it obviously also satisfies equation (12). Zero solution corresponds to a state when the conductor is not connected to the source. In model 2, i.e. model 2I or model 2J, the current density $J(r, t)$ in a conductor is determined by the functions $J_k(t), k = 1, 2, \ldots, n$. If some current density $J(r, t)$ is the solution of model 1 or model 2, then any multiple of this current density is also the solution of the respective model. Every solution of model 2I or model 2J can be normalized using $\underline{J_s}$. It is easy to prove that for given κ, n and s, such normalized solutions of models 2I and 2J are identical to the solution of model 2J normalized with respect to $\underline{J_s}$.

Every $r \in [r_\mathrm{i}, r_\mathrm{o}]$ lies in some partial interval $[r_{k-1}, r_k]$. Using the notation introduced in this paper, we can thus write $J(r, t) = J_k(t)$ and

$$B(r, t) = \sum_{\ell=1}^{n} J_\ell(t)\mathscr{B}_\ell(r).$$

For $c_k = r$ and $c_{k+1} = r + \Delta r$, equation (17) can be written in the form

$$J(r + \Delta r, t) - J(r, t) - \gamma \frac{\partial}{\partial t} \int_r^{r+\Delta r} B(r, t)\,\mathrm{d}r = 0. \tag{21}$$

The magnetic field in the conductor is continuous and therefore the mean value theorem [7, 11] can be applied, according to which

$$\int_r^{r+\Delta r} B(r, t)\,\mathrm{d}r = \Delta r B(r + \theta\Delta r, t), \qquad \theta \in (0, 1),$$

and equation (21) can be written in the form

$$\frac{J(r + \Delta r, t) - J(r, t)}{\Delta r} - \gamma \frac{\partial}{\partial t} B(r + \theta\Delta r, t) = 0.$$

For $\Delta r \to 0$, this equation converges to the equation

$$\frac{\partial J}{\partial r} - \gamma \frac{\partial}{\partial t} B(r, t). \tag{22}$$

In this equation we express $B(r, t)$ in terms of (1) and (5), differentiate the equation with respect to r, and after some rewriting we obtain equation (9). This result increases the probability that the two models considered are correct, but it poses a question: is it necessary to deal with model 2 described by equations (17) and (18) when there exists model 1 described by the elegant equation (9)? Moreover, the solution of equation (9) is also expressed explicitly by formula (13) if the conductor is supplied by sinusoidal current.

According to [7, 12, 13], equation (12) has in the interval $[\kappa r_\mathrm{i}, \kappa r_\mathrm{o}]$ a unique solution $\underline{J^x}(x)$, which satisfies the initial conditions

$$\underline{J^x}(X) = Y_0, \qquad \frac{\mathrm{d}}{\mathrm{d}x}\underline{J^x}(X) = Y_1,$$

where X, Y_0 and Y_1 are the given numbers, $X \in [\kappa r_\mathrm{i}, \kappa r_\mathrm{o}]$. The unique solution is given by relation (13), in which the constants c_B and c_K are determined using the initial conditions. According to subsection 2.1, the phasor of current density $\underline{J}(r)$ is the solution of equation (10) on the interval $[r_\mathrm{i}, r_\mathrm{o}]$, where $r_\mathrm{i} > 0$, and it holds

$$\underline{J}(r) = c_B[\mathrm{ber}(\kappa r) + \mathrm{j}\,\mathrm{bei}(\kappa r)] + c_K[\mathrm{ker}(\kappa r) + \mathrm{j}\,\mathrm{kei}(\kappa r)], \tag{23}$$

with the constants c_B and c_K being the solution of a system of linear equations:

$$c_B[\mathrm{ber}(\kappa \bar{r}) + \mathrm{j}\,\mathrm{bei}(\kappa \bar{r})] + c_K[\mathrm{ker}(\kappa \bar{r}) + \mathrm{j}\,\mathrm{kei}(\kappa \bar{r})] = p, \tag{24}$$

$$c_B[\mathrm{ber}'(\kappa\bar{r}) + \mathrm{j}\,\mathrm{bei}'(\kappa\bar{r})] + c_K[\mathrm{ker}'(\kappa\bar{r}) + \mathrm{j}\,\mathrm{kei}'(\kappa\bar{r})] = \frac{d}{\kappa}, \tag{25}$$

where the apostrophe denotes derivatives with respect to x, and

$$\underline{J}(\bar{r}) = p, \qquad \frac{\mathrm{d}}{\mathrm{d}r}\underline{J}(\bar{r}) = d, \tag{26}$$

with $\bar{r}$, p and d being the given numbers $\bar{r} \in [r_\mathrm{i}, r_\mathrm{o}]$.

Choosing the numbers $\bar{r}$ and p is no problem; the problem is to choose *a priori* the number d. The first condition in (26) is matched in model 2J by the choice of current density $J_s(t)$, while the second condition in (26) is a price for differentiating. Model 2 starts from integral relations (1) and (2), whereas model 1 starts from differential relations (6) and (7). In the above proof of the equivalence of the two models, equation (9), which represents model 1, is obtained from equation (22) of model 2 by differentiating with respect to r. A consequence of every differentiation is the loss of information, and this information has to be complemented. In model 1, this complementation is the second condition in (26).

4. Examples

In all the examples given below it is assumed that the total current through the conductor (see (18)) is $I = \sin\omega t$, i.e.

$$\underline{I} = \hat{I}, \qquad \hat{I} = 1\mathrm{A}.$$

In agreement with (19), the phasor of current density in conductor $\underline{J}(r)$ is given by the numbers $\hat{J}_k$ and α_k, $k = 1, 2, \ldots, n$, which are obtained by solving equations (20) and (18). In the following figures, the normalized amplitude of the current density $J_\mathrm{rel} = J_\mathrm{rel}(r)$ is shown as a curve joining the points $(c_k, \hat{J}_k/J_\mathrm{max})$, where

$$J_\mathrm{max} = \max_{k=1,2,\ldots,n} \hat{J}_k.$$

The initial phase angle α_k of the current density in the kth partial conductor in the figures is shown as a curve $\alpha(r)$ joining the points (c_k, α_k). The points $c_k, k = 1, 2, \ldots, n$, (see subsection 2.2) were chosen as follows:

$$c_k = r_k + (r_k - r_{k-1})\left[\Theta + \frac{k-1}{n-1}(1-\Theta)\right], \qquad \Theta \in [0, 1]. \tag{27}$$

With this choice, it holds $c_n = r_\mathrm{o}$ and $J_\mathrm{max} = \hat{J}_n$. The calculated current density is practically independent of Θ and n if $n \geqslant 200$. The resistivity values at a temperature of 293 K, which is used in examples, were taken over from [14]

Metal	ϱ (10^{-8} Ωm)
Silver (Ag)	1.587
Copper (Cu)	1.678
Aluminium (Al)	2.650
Platinum (Pt)	10.5

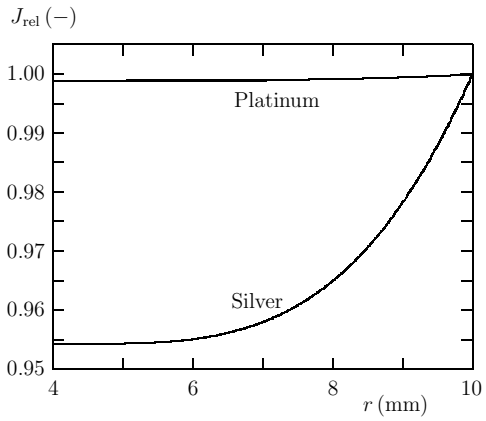

Figure 2. Normalized amplitude of current density in a conductor cross-section in example 1.

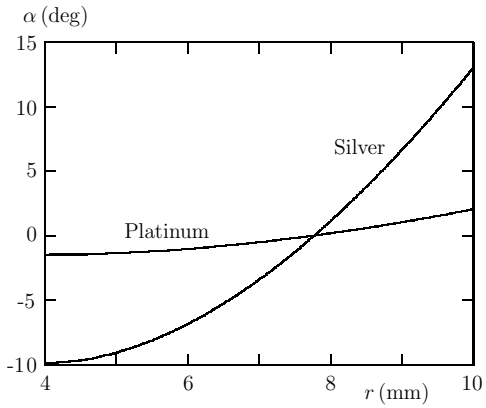

Figure 3. Initial phase of current density in a conductor cross-section in example 1.

4.1. Example 1

A silver or platinum tubular conductor is 8 mm in inner diameter ($r_{\mathrm{i}} = 4$ mm) and 20 mm in outer diameter ($r_{\mathrm{o}} = 10$ mm); the angular frequency of the current source $\omega = 2\pi f$, where $f = 60$ Hz.

The calculated dependence of the normalized amplitude J_{rel} and of the initial phase α of the current density on the distance r from the conductor axis is shown in figure 2 and in figure 3, respectively. The normalized amplitude of current density in figure 2 is the solution of model 2I. The same values as in figure 2 would be obtained by normalizing the solution of model 2J or by solving model 2J for

$$\underline{J_s} = \underline{J_n} = \exp(\mathrm{j}\,\alpha_n),$$

where $\alpha_n = \alpha(r_{\mathrm{o}})$ in figure 3. When choosing $\underline{J_s} = \underline{J_n}$ with the initial phase $\alpha'_n \neq \alpha_n$, the curve $\alpha(r)$ will be shifted in parallel such that $\alpha(r_{\mathrm{o}}) = \alpha'_n$. The dependence of the curve $\alpha(r)$ on the choice of the angle of phasor $\underline{J_s}$ does not indicate any ambiguity of the solution of model 2J; it is merely the choice of the instant $t = 0$. It holds

$$\sin(\omega t + \alpha_n) = \sin(\omega t' + \alpha'_n)$$

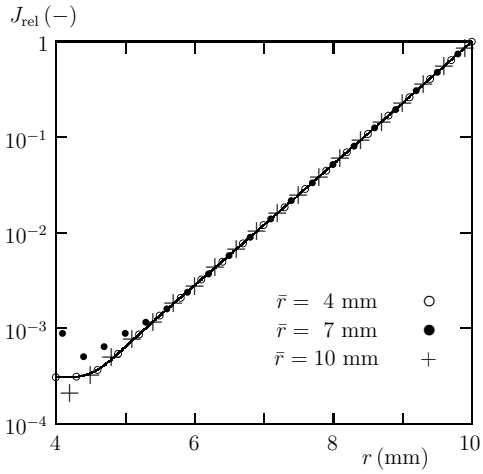

Figure 4. Normalized amplitude of current density in the cross-section of a conductor in example 2 obtained via solving model 2 (solid line) and model 1 (isolated points) for differently chosen initial conditions.

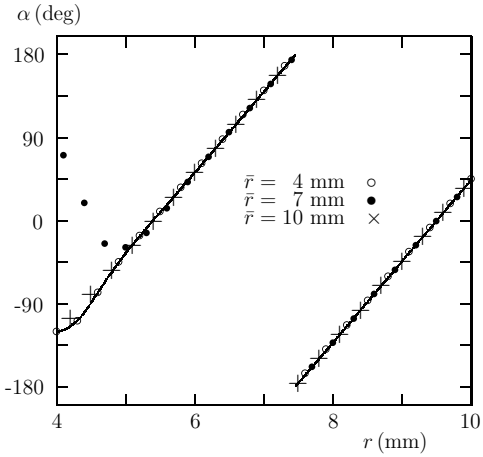

Figure 5. Initial phase of current density in the cross-section of conductor in example 2 obtained via solving model 2 (solid line) and model 1 (isolated points) for differently chosen initial conditions.

for

$$t' = t + \frac{\alpha_n - \alpha'_n + 2\vartheta\pi}{\omega},$$

where ϑ is an integer. Likewise, the solution of model 2I is affected by the choice of the angle of phasor $\underline{I}$.

4.2. Example 2

A copper conductor of the same dimensions as in example 1 is supplied from a source of frequency $f = 10$ kHz.

The current density in the conductor, shown in figures 4 and 5, was obtained via solving model 2I for $n = 500$, $\Theta = 0$. Using this solution, complex numbers p and d can be determined

for any arbitrary chosen $\bar{r} \in [r_\mathrm{i}, r_\mathrm{o}]$ that satisfy relation (26), and by solving equations (24) and (25) c_B and c_K can be obtained. This in fact determines the solution of (23) of model 1. Several isolated points of the solution of model 1 are illustrated in figures 4 and 5 for three different values of $\bar{r}$. The curve $\alpha(r)$ in figure 5 has one discontinuity point. This discontinuity is only apparent since the phasor angle is adjusted such that it holds $\alpha \in (-180, 180]$ deg. The number of points of apparent discontinuity increases with increasing f. Equation (12) is linear with respect to the derivatives and its solution is defined for at least $r \in [r_\mathrm{i}, r_\mathrm{o}]$. According to [7] $\bar{r}$ can be chosen anywhere in the interval $[r_\mathrm{i}, r_\mathrm{o}]$, but figures 4 and 5 do not testify to this. In section 3, it was proved exactly that the two models were equivalent. The discrepancy between the solutions of model 2 and model 1 for $\bar{r} = 7$ mm and 10 mm can only be explained by the sensitivity of model 1 to initial conditions and by the fact that the value d was obtained by numerical differentiation of discrete data obtained by the solution of model 2. The differentiation of numerical data does not exactly belong to precise numerical operations [15]. On this occasion, attention should also be drawn to potential problems in the calculation of the current density phasor using formula (13) since the calculation of the values of Kelvin functions is for higher values of x numerically unstable. For example, the calculation of the functions ker and kei by simply adding up the series in terms of which these functions are defined is in d.p. (double precision) unstable already for $x > 12$. For a copper conductor and $r = 10$ mm we have, by (11), $x > 12$ already for $f > 3.2$ kHz. In the present work therefore, asymptotic formulae are used that are given in [16]. The problems of calculating the Kelvin functions have also attracted attention quite recently, as witnessed by Mingli *et al* [3, 17].

4.3. Example 3

An aluminium tubular conductor is 16 mm in inner diameter and 20 mm in outer diameter; the current source frequency is $f = 1$ MHz to 1 GHz.

In the present paper it is assumed that the vectors $\boldsymbol{J}$ and $\boldsymbol{B}$ do not depend on the z coordinate, i.e. the current is considered to be slowly varying (according to [5]). This restriction can be met by requiring that the maximum linear dimension of the system, ℓ_max, be much smaller than the free space wavelength associated with the driving frequency. That is

$$f \ll \frac{c}{\ell_\mathrm{max}},$$

where c is the speed of light in vacuum. By this criterion and for $\ell_\mathrm{max} = 0.1$ m, the frequency 1 GHz is at the upper limit of the applicability of models 1 and 2.

The calculated dependence of the normalized amplitude J_rel and the initial phase α of current density on distance r from the conductor axis is shown in figures 6 and 7, respectively. The magnitude of J_rel in the right neighbourhood of point r_i decreases with increasing f. With increasing f, the condition number [18] of matrix $\boldsymbol{M}_\mathrm{I}$ or $\boldsymbol{M}_\mathrm{J}$ of the system of linear equations of model 2I or model 2J also increases. Roughly speaking, the condition number of matrices $\boldsymbol{M}_\mathrm{I}$ and $\boldsymbol{M}_\mathrm{J}$ increases with increasing f and r_o, and with decreasing r_i. With an increasing condition number, matrices $\boldsymbol{M}_\mathrm{I}$ and $\boldsymbol{M}_\mathrm{J}$ become ill-conditioned [15], and in the numerical calculation the result of the calculation may be distorted due to rounding errors or, in the extreme case, matrices $\boldsymbol{M}_\mathrm{I}$ and $\boldsymbol{M}_\mathrm{J}$ cannot be inverted. The calculation precision is given by the number of bits reserved in the computer for representing a real number. Usually it is 64 bits, and this precision is called d.p. In a calculation with the given precision there may be problems if some values $\hat{J}_k/J_\mathrm{max}$ are comparable with the machine epsilon, which is the minimum number that is not negligible with respect to the number 1. In d.p., the machine epsilon is equal to 2^{-52}. There will certainly be problems in the calculation if some values $\hat{J}_k/J_\mathrm{max}$ are comparable with the least number that is represented in the computer as non-zero;

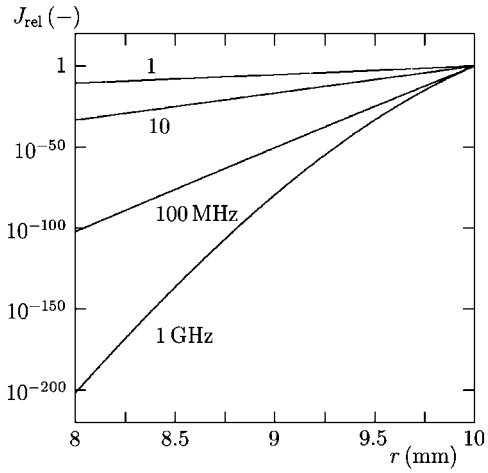

Figure 6. Normalized amplitude of current density in the cross-section of a conductor in example 3.

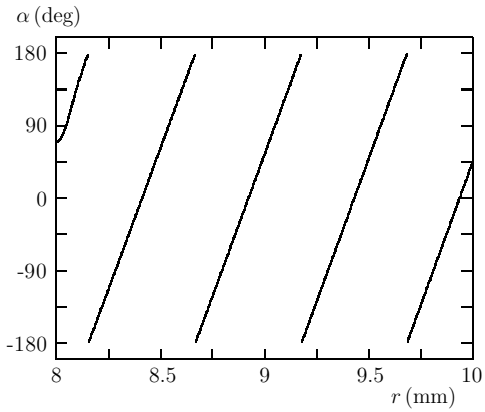

Figure 7. Initial phase of current density in the cross-section of a conductor in example 3 for $f = 1$ MHz.

in d.p. it is 2^{-1022}. In figure 6, the curves for $f > 1$ MHz show the solution obtained by calculation with greater precision than d.p. In figure 6, the result of numerical calculation is plotted irrespective of the possibility of realizing the large range of current density.

5. Current density in a cylindrical conductor

The cylindrical conductor is a tubular conductor with zero inner diameter, i.e. $r_{\mathrm{i}} = 0$. Model 1 is expressed by equation (12) and its solution (13) for initial conditions (26). Equation (12) was derived for $r_{\mathrm{i}} > 0$ and thus its application to calculate current density in the cylindrical conductor is not quite correct without some detailed reasoning. The point $x = 0$, where $x = \kappa r$, is the singular point of equation (12). This singularity can, however, be

removed because the limit of all three members on the left side of equation (12) is finite for $x \to 0+$.

We will show that the solution of model 1 for the cylindrical conductor is given by the relation

$$\underline{J}(r) = c_B[\mathrm{ber}(\kappa r) + \mathrm{j}\,\mathrm{bei}(\kappa r)], \qquad c_B = \frac{p}{\mathrm{ber}(\kappa \bar{r}) + \mathrm{j}\,\mathrm{bei}(\kappa \bar{r})}, \tag{28}$$

where p is the chosen current density factor at a distance $\bar{r}$ from the conductor axis; $\bar{r} \geqslant 0$. Solution (28) corresponds to the solution of model 2J for a given $J_s(t)$, with $\bar{r}$ lying in the sth partial conductor.

Proof. In the proof of the statement, we will consider the initial conditions

$$\underline{J}(\bar{r}) = p, \qquad \frac{\mathrm{d}}{\mathrm{d}r}\underline{J}(\dot{r}) = d, \qquad \bar{r}, \dot{r} \in [0, r_\mathrm{o}],$$

which are more general than conditions (26). We choose a sequence of tubular conductors such that r_i gradually decreases, and $r_\mathrm{i} \to 0+$. For each tubular conductor we always choose $\dot{r} = r_\mathrm{i}$, while we consider $\bar{r}$ to be chosen fixed if $\bar{r} \geqslant r_\mathrm{i}$. In case $\bar{r} < r_\mathrm{i}$, we will choose $\bar{r} = r_\mathrm{i}$. Proceeding like this is not in contradiction with $\bar{r}$ being given *a priori* since in the examination of the given sequence of tubular conductors, what is of importance is the state when the limit is reached. There are two possibilities: either $\bar{r} > 0$ or $\bar{r} = 0$. For $\bar{r} > 0$, a finite number of steps must lead to $\bar{r} \geqslant r_\mathrm{i}$. If $\bar{r} = 0$, this equality occurs exactly in the limit. According to section 3, the constants c_B and c_K are the solutions of the equations

$$c_B[\mathrm{ber}(\kappa \bar{r}) + \mathrm{j}\,\mathrm{bei}(\kappa \bar{r})] + c_K[\mathrm{ker}(\kappa \bar{r}) + \mathrm{j}\,\mathrm{kei}(\kappa \bar{r})] = p, \tag{29}$$

$$c_B[\mathrm{ber}'(\kappa \dot{r}) + \mathrm{j}\,\mathrm{bei}'(\kappa \dot{r})] + c_K[\mathrm{ker}'(\kappa \dot{r}) + \mathrm{j}\,\mathrm{kei}'(\kappa \dot{r})] = \frac{d}{\kappa}, \tag{30}$$

where the apostrophe denotes derivatives with respect to $x = \kappa r$. For $r_\mathrm{i} \to 0+$ the functions $\mathrm{ber}'(\kappa \dot{r})$, $\mathrm{bei}'(\kappa \dot{r})$ and $\mathrm{kei}'(\kappa \dot{r})$ converge to zero since $\dot{r} = r_\mathrm{i}$. Thus by (30)

$$c_K \to \frac{d}{\kappa\,\mathrm{ker}'(\kappa \dot{r}))},$$

and this means that $c_K \to 0$ because

$$\lim_{\dot{r} \to 0+} \mathrm{ker}'(\kappa \dot{r}) = -\infty.$$

This also proves that $c_K = 0$ for the cylindrical conductor and the validity of (28) follows from (23) and (29). Let us only add that for $\bar{r} = 0$, the relation $c_B = p$ holds because $\mathrm{ber}(0) = 1$ and $\mathrm{bei}(0) = 0$.

An idea of the effect of the magnitude of n on the solution of model 2 can be formed by comparing the solutions of models 1 and 2 for the cylindrical conductor. Figure 8 gives a part of the solution of models 1 and 2J for an aluminium conductor of 20 mm in diameter, $f = 10^5$ Hz. Both models were solved on the assumption that $\underline{J}(r_\mathrm{o}) = 1$ A m^{-2}; their solution differs the most in the neighbourhood of the longitudinal conductor axis. This magnitude of deviation depends on n and Θ. Shown in figure 8 is the $\hat{J}(r)$ amplitude of the solution of model 1 in the neighbourhood of point $r = 0$ by a continuous curve, and the solution of model 2J is illustrated by amplitudes $\hat{J}_k$ for several values of n. When calculating the solution of model 2J, $\Theta = 0.5$ was chosen in formula (27). Let us add that the convergence of the solution of model 2 to the solution of model 1 worsens with increasing frequency f.

Figure 9 illustrates the normalized phasor $\underline{J}_\mathrm{rel} = \underline{J}/J_\mathrm{max}$ in Gaussian plane for several frequencies in a cylindrical aluminium conductor of 20 mm in diameter. For $f = 0$ the current density in the conductor cross-section is constant, $\underline{J}_\mathrm{rel}(r) = 1$, and its normalized

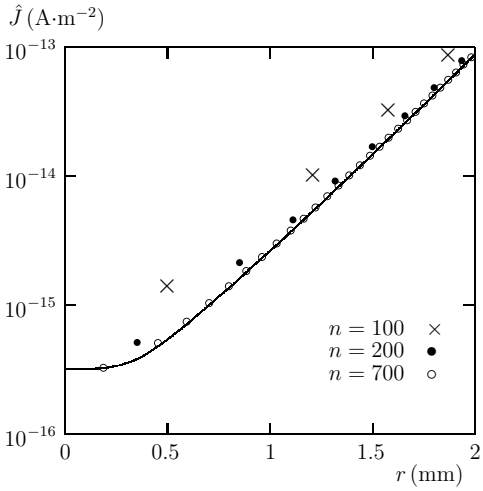

Figure 8. Amplitude of the solution of models 1 (solid line) and 2J (isolated points) in the neighbourhood of a longitudinal conductor axis.

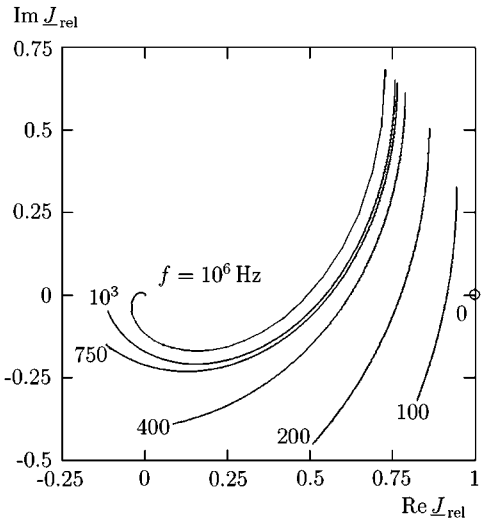

Figure 9. Normalized phasor of the solution of model 2J in Gaussian plane in dependence on the frequency of the source.

phasor is shown as a point marked with a circle. If $f > 0$, then each curve in figure 9 begins at the point $\underline{J}_{\mathrm{rel}}(r_{\mathrm{o}})$, at which it holds $|\underline{J}_{\mathrm{rel}}(r_{\mathrm{o}})| = 1$, and it ends at the point $\underline{J}_{\mathrm{rel}}(0)$. The argument of current density phasor in the cylindrical conductor has a similar course as in the tubular conductor (see figures 3, 5 and 7). The curve for $f = 10^6$ Hz forms a spiral in the neighbourhood of the beginning of the Gaussian plane, which runs several times round the beginning. This spiral cannot be seen in figure 9 because for $r < 9.239$ mm the module of phasor $\underline{J}_{\mathrm{rel}}$ is in the interval $(10^{-52}, 10^{-4})$ and therefore the spiral blends in with the beginning of the Gaussian plane.

6. Conclusion

In the paper, two models are described whose solution is the current density in an isolated tubular conductor supplied by an ideal current source with a frequency not exceeding 1 GHz. It is proved in section 3 that the two models are equivalent. For the source of sinusoidal current, model 1 is represented by equation (12), by its general solution (13) and by initial conditions (26). Models 2I and 2J are in principle formed by a system of linear equations (19) and by the condition placed on the total conductor current or on the current density. Model 1 cannot be used in the case that $r_i > 0$ because d in (26) cannot be determined *a priori*. It was shown in section 5 that for the cylindrical conductor in the general solution, (13), the constant c_K is equal to zero and thus model 1 is in this case useable.

The proposed general methods are used on several actual examples of tubular and cylindrical conductors. The solutions of examples are given in the figures. When solving the examples, much attention is devoted to the problem associated with the realization of numerical calculation on a computer.

Acknowledgments

In the first place, I would like to express my gratitude to MUDr Ivo Šabacký from St. Anne's University Hospital in Brno. Thanks to his treatment, I am still alive and can work. This paper contains solution results of the Research plan no MSM0021630516 of the Ministry of Education, Youth and Sports of the Czech Republic.

References

[1] Shenkman A L 1998 *Circuit Analysis for Power Engineering Handbook* (Dordrecht: Kluwer)
[2] Miranda E N 1999 A simple model for understanding the skin effect *Int. J. Elect. Eng. Educ.* **36** 31–6
[3] Mingli W and Yu F 2004 Numerical calculations of internal impedance of solid and tubular cylindrical conductors under large parameters *IEE Proc.* C **151** 67–72
[4] Coufal O 2007 Current density in a pair of solid coaxial conductors *Electromagnetics* **27** 299–320
[5] Reitz J R, Milford F J and Christy R W 1993 *Foundations of Electromagnetic Theory* (Reading, MA: Addison-Wesley)
[6] Haňka L 1975 *Electromagnetic Theory* (Prague: SNTL) (in Czech)
[7] Rektorys K and Vitásek E (ed) 1994 *Survey of Applicable Mathematics* vols 1 and 2 (Dordrecht: Kluwer)
[8] Maxwell J C 1954 *A Treatise on Electricity and Magnetism* vol 2, Unabridged 3rd edn (New York: Dover)
[9] Weisstein E W 2002 *CRC Concise Encyclopedia of Mathematics* 2nd edn (Boca Raton, FL: CRC Press)
[10] Hairer E and Wanner G 1996 *Solving Ordinary Differential Equations II* (Berlin: Springer)
[11] Sobolev S L 1989 *Partial Differential Equations of Mathematical Physics* (New York: Dover)
[12] Kamke E 1965 *Ordinary Differential Equations* (Moscow: Nauka) (in Russian)
[13] Matveĭev N M 1960 *Collection of Examples on Ordinary Differential Equations* (Leningrad: University of Leningrad Publishing House)
[14] Lide D R 2007 *CRC Handbook of Chemistry and Physics* 88th edn (New York: CRC Press)
[15] Ralston A and Rabinowitz P 2001 *A First Course in Numerical Analysis* (Mineola, New York: Dover)
[16] Springer Online Reference Works 2002 *Encyclopedia of Mathematics* (Berlin: Springer) http://eom.springer.de/
[17] Brualla L and Martin P 2001 Analytic approximations to Kelvin functions with applications to electromagnetics *J. Phys. A: Math. Gen.* **34** 9153
[18] Young D M 1971 *Iterative Solution of Large Linear Systems* (New York: Academic)